ROBUST MODEL-BASED CONTROLLER SYNTHESIS FOR THE SCOLE CONFIGURATION

E. S. ARMSTRONG AND S. M. JOSHI
SPACECRAFT CONTROLS BRANCH
NASA LANGLEY RESEARCH CENTER
HAMPTON, VA 23665-5225

AND

E. J. STEWART
GEORGE WASHINGTON UNIVERSITY
HAMPTON, VA 23665

Robust Model-Based Controller Synthesis for the SCOLE Configuration

E.S. Armstrong S.M. Joshi E.J. Stewart*

NASA Langley Research Center
Hampton, VA 23665

ABSTRACT

The design of a robust compensator is considered for the SCOLE configuration using a frequency-response shaping technique based on the LQG/LTR algorithm. Results indicate that a tenth-order compensator can be used to meet stability-performance-robustness conditions for a 26th-order SCOLE model without destabilizing spillover effects. Since the SCOLE configuration is representative of many proposed spaceflight experiments, the results and design techniques employed potentially should be applicable to a wide range of large space structure control problems.

Introduction

Large space structures (LSS) have many properties that make them difficult to analyze and control [1]. They are mathematically modeled by computationally difficult partial differential equations or high-order, lumped, ordinary differential equations obtained through finite element methods. LSS have many low and closely spaced resonant frequencies, a number of which typically fall within the controller bandwidth. In LSS, vibrational issues must be treated as a first-order effect; it is this characteristic of the LSS control problem that most distinguishes it from spacecraft control problems of the past. Additionally, inherent damping is low and/or improperly modeled. Coupled with stringent operational requirements for orientation, shape control, and vibration suppression, these properties present an unconventional and unresolved control design problem to the system analyst.

A fundamental issue to be dealt with in any LSS control problem comes from the large amount of modeling error occurring in finite element models of such structures. In general, inaccuracy of modal data, such as elastic frequencies and mode shapes used to form coefficient matrices of the dynamic models, increases with increasing modal frequency. Hence, a frequency-dependent constraint is inherently imposed on the design process in that stabilization and performance requirements must be met without allowing the input control energy to "spill-over" and excite and destabilize the lightly damped, poorly modeled high-frequency dynamics.

At NASA's Langley Research Center, a LSS configuration known as the Spacecraft Control Laboratory Experiment (SCOLE) was conceived for the purpose of evaluating and comparing large space structure control and identification concepts [2]. The SCOLE configuration (shown schematically in Figure 1) consists of a 130-foot flexible beam anchored at one end to the cargo bay of the space shuttle with an antenna reflector connected to the opposite end. The center of mass of the reflector is offset from the attachment point. The SCOLE configuration is representative of many proposed space flight experiments and space-based antenna systems. Control inputs are available from torque actuators located on the orbiter and force actuators at the reflector center. Attitude sensors are located at the reflector center. A typical SCOLE control task is to slew or change the line-of-sight of the antenna rapidly and damp any induced structural vibrations to the degree required for the precise pointing of the antenna.

In this paper we consider a SCOLE large-angle slewing maneuver to have been completed and attack the problem of designing a model-based compensator to attenuate residual structural vibrational motion and antenna line-of-sight error. The SCOLE mathematical model is first discussed followed by descriptions of the design objectives and the compensator design approach. Finally, results from the application of the design methodology to the SCOLE problem are presented.

Mathematical Model

The basic distributed-parameter mathematical model of the SCOLE configuration is described in [2], while nonlinear and linear ordinary differential equation models are found in [3] and [4], respectively. A linear finite-element model consisting of three rigid rotational modes and the first ten structural elastic modes is used in this study. A state-space realization of the modal model has the

* George Washington University, Hampton, VA

form

$$\dot{x}_F = A_F x_F + B_F u \tag{1}$$

$$y_F = C_F x_F \tag{2}$$

where

$$A_F = \text{diag}(A_R, A_E) \tag{3}$$

$$A_R = \begin{bmatrix} 0 & I_3 \\ 0 & 0 \end{bmatrix}_{6\times6} \tag{4}$$

$$A_E = \text{diag}(A_E^1, A_E^2, \ldots, A_E^{10}) \tag{5}$$

and

$$A_E^i = \begin{bmatrix} 0 & 1 \\ -\omega_i^2 & -2\zeta_i\omega_i \end{bmatrix}_{2\times2} \tag{6}$$

for (i=1,...,10). Equation (4) describes the rigid body contribution and equations (5) and (6) describe the elastic contribution for ten vibrational modes of frequencies ω_i, (i = 1,..., 10). A uniform damping ratio of $\zeta_i = \zeta = 0.003$, (i = 1,..., 10), is assumed. The eigenvalues of A_E are given mathematically by

$$\lambda_i = -\zeta\omega_i \mp j\,\omega_i\sqrt{1-\zeta^2} \tag{7}$$

and are shown in Table I.

Five control inputs are generated using three torque actuators (one per X,Y,Z axis) on the orbiter and two force actuators (X and Y directions in Figure 1) at the reflector center. Three attitude sensors (one per axis) are located at the reflector center. Sensor and actuator dynamics were not included in this study. Rigid-body inertias, mode shape and slope data from the finite element analysis combine to define the control effectiveness matrix B_F and output response matrix C_F.

Analysis of (1) and (2) verifies that the system is completely controllable and observable. Attempts to reduce the number of control variables to the number of outputs retained controllability and observability but, in each three-control input combination, introduced lightly-damped, low-frequency transmission zeros [5] into the model. Since the presence of such transmission zeros has been demonstrated to reduce system performance in large space structure controller designs [6], the compensator was designed with the original five inputs and three outputs. However, in order to avoid numerical ill-conditioning brought about by the different physical characteristics of forces and torques, the inputs were scaled so that the frequency response of the largest ($\bar{\sigma}(j\omega)$) and smallest ($\underline{\sigma}(j\omega)$) singular values of the transfer matrix of (1) and (2), denoted by $G_F(j\omega)$, were nearly equal at low frequencies (as shown in Figure 2).

Design Objectives

The design objectives of this study are to produce a multivariable, model-based, feedback compensator operating on attitude sensor data which will generate force and torque inputs to stabilize the rigid body modes; enhance the stability of lightly damped, low-frequency modes without destroying the stability of higher-frequency modes; meet prescribed closed-loop performance (bandwidth) specifications; and possess some degree of stability robustness to unmodeled dynamics. Since a low-order controller is sought, it was decided to employ full-state controller design with a reduced-order plant model. The full-order model is reserved for evaluation purposes. Order reduction for the design plant was performed using modal truncation. Past studies ([6], [7]) have indicated that a 0.1 rad/sec closed-loop performance bandwidth is sufficient to maintain antenna pointing control, and a design model composed of the rigid body plus the first three elastic modes in Table I is adequate to achieve this bandwidth. Higher bandwidths will typically require the addition of extra elastic modes to the design model. Denoting the 12th-order design model transfer matrix by $G_p(s)$, for a unity-gain feedback compensator with transfer matrix $G_c(s)$, multivariable bandwidth will be defined as the frequency below which the smallest singular value of the closed-loop response matrix

$$G_{CL}(s) = G_p(s)G_c(s)[\ I + G_p(s)G_c(s)\ ]^{-1} \tag{8}$$

remains above unity for $s = j\omega$. In our case, we seek a compensator such that

$$\underline{\sigma}[G_{CL}(j\omega)] \geq 1.0 \text{ for } 0 \leq \omega \leq 0.1 \tag{9}$$

From the block diagonal structure of A_F in (1), the transfer matrix, $G_F(s)$, of the 26th-order system may now be written as

$$G_F(s) = G_p(s) + \Delta G(s) \tag{10}$$

where $\Delta G(s)$ represents the transfer matrix of the remaining 14th-order (residual) modal system. In this form, the dynamics represented by $\Delta G(s)$ can be interpreted as an "additive perturbation" to the $G_p(s)$ system and used as an approximate representation of unmodeled dynamics for use in stability robustness tests. Specifically, it is established in [8] that the unmodeled dynamics $\Delta G(s)$ will not destroy the closed-loop stability so long as

$$\bar{\sigma}[\ G_c(s)[\ I + G_p(s)G_c(s)\ ]^{-1}\ ]\ \bar{\sigma}[\Delta G(s)] \leq 1 \tag{11}$$

for all $s = j\omega$, ω real. Condition (11) can be enforced in the compensator design stage to ensure that closed-loop stability will be preserved for at least that class of unmodeled dynamics whose spectral norm lies below $\bar{\sigma}[\Delta G(j\omega)]$.

The spillover effect on $\Delta G(s)$ due to the closed-loop compensation may be tested directly by applying a state-variable realization of $G_c(s)$ to the full 26th-order model given by (1) and (2) and examining the eigenvalues of the composite system.

A block diagram for the closed-loop configuration is shown in Figure 3. An approach for constructing $G_c(s)$ to stabilize $G_p(s)$ while satisfying (9) and (11) is presented in the next section.

Compensator Design Approach

The compensator design approach employed to meet the foregoing design objectives can be viewed as a variation of the well-known Linear-Quadratic-Gaussian/Loop-Transfer-Recovery (LQG/LTR) algorithm ([9], [10]). In the standard LQG/LTR approach, with the loop in Figure 3 broken at the output, a Kalman filter (G_{KF}) is designed to meet the complete set of stability-performance-robustness objectives. Thereafter, an optimal linear regulator is constructed such that the composite LQG compensator (G_c) loop gain behavior asymptotically approaches (recovers) that of G_{KF} in the sense that

$$G_p(j\omega)G_c(j\omega) \rightarrow G_{KF}(j\omega)$$

pointwise in ω. Direct application of this LQG/LTR procedure to large space structures problems results in extremely conservative designs which cannot meet reasonable performance specifications [6]. However, the LQG/LTR structure still provides a viable approach for model-based controller synthesis when the standard procedure is modified in the following manner.

Step 1
Denote a state-variable realization of $G_p(s)$ by

$$\dot{x} = Ax + Bu \tag{12}$$

$$y = Cx \tag{13}$$

Select the design parameters L and μ in the Kalman filter algorithm

$$AQ + QA^T + LL^T - \frac{1}{\mu} QC^TCQ = 0 \tag{14}$$

$$H = \frac{1}{\mu} QC^T \tag{15}$$

such that

$$G_{KF}(s) = C(sI-A)^{-1}H \tag{16}$$

achieves a desired (target) loop gain for $G_p(s)G_c(s)$ over some low-frequency band containing the design bandwidth.

Step 2
By successively increasing $q > 0$ in equation (19) (to follow), design an optimal linear regulator which, when used in an LQG fashion with the Kalman filter from *Step 1*, asymptotically recovers the frequency response of the target loop gain over the low-frequency band. The resulting compensator is given by

$$G_c(s) = F(sI-\hat{A})^{-1}H \tag{17}$$

where

$$F = B^TP \tag{18}$$

$$A^TP + PA - PBB^TP + qC^TC = 0 \tag{19}$$

$$\hat{A} = A-BF-HC \tag{20}$$

Step 3
Attempt to adjust q in *Step 2* until the desired bandwidth condition (condition (9)) is met. Also check stability robustness by (11). If an excessively high q (indicated by violation of (11)) is required to achieve the required bandwidth, turn down the Kalman filter gain (by increasing μ in (14)) to "loosen" the target loop. In effect, this procedure reduces the target bandwidth until satisfaction of (11) is possible. The final design is accomplished by iteratively adjusting the linear regulator and Kalman filter design parameters until an appropriate compromise is made between bandwidth and stability robustness.

In large space structures applications, the inability (at *Step 1*) to meet loop gain magnitude over the desired bandwidth or (in *Step 3*) the production of too small a compromise bandwidth can often be overcome by the inclusion of additional flexible modes into the design model [6].

If, as in the SCOLE application to follow, an order-reduction study is performed on the resulting compensator, the complete set of stability-performance-robustness conditions needs to be re-evaluated with the reduced-order compensator.

SCOLE Application

Figure 4 shows the frequency response of the 12th-order (LQG) compensator, G_c, resulting from an application of the foregoing procedure to the 12th-order SCOLE design model, G_p. The figure indicates a well-behaved lead-lag structure with a 20 db/decade roll-off. Eigenvalues of the corresponding A-HC, A-BF, and $\hat{A}$ matrices are given in Table II. The frequency response of G_{CL} in equation (8) with the 26th-order evaluation model used in place of G_p is shown in Figure 5. Figure 5 demonstrates the satisfaction of the 0.1 rad/sec bandwidth requirement and a 60 db/decade roll-off. Eigenvalues of the composite system resulting from the LQG compensator applied to the evaluation model are given in the first column of Table III. The data indicate that the compensator was designed to concentrate on stabilizing the rigid body modes (first three entries of the A-HC block) without disturbing the stability of the three elastic modes (last three entries of the A-HC block) of the

design model. Table III also shows that there is insignificant spillover into ΔG. The stability robustness test (11) shown in Figure 6 shows more than 10 db robustness margin.

The possibility of a reduced-order compensator (ROC) satisfying the design conditions was also investigated. The methods of balanced realization [11], Hankel-norm reduction [12] and a method based on stable factorization [13] were employed. The ratio of largest to smallest Hankel singular values was 0.016 so little reduction based on nearly uncontrollable or unobservable compensator modes was expected. All of the methods gave similar results. In each order reduction method, only a 10th-order ROC would stabilize the design model. The stable factorization results were judged to be (slightly) better and will be discussed herein.

Table II shows the eigenvalues of the corresponding $\hat{A}$ matrix in the ROC, denoted by $\hat{A}_{ROC}$. Figure 7 shows a frequency response of the ROC. A comparison of Figures 4 and 7 shows that the only difference between the LQG and ROC frequency response plots is the removal of the dip in $\underline{\sigma}$ at the frequency of the third elastic mode. The importance of this characteristic can be seen from Figure 8 where the robustness condition (11) is evaluated using the ROC in place of G_c. Figure 8 indicates that an effect of the-order reduction is a reduction of stability margin at the frequency of the third elastic mode. A more positive effect from the reduced order compensation is seen in the second column of Table III where the eigenvalues of the ROC applied to the evaluation model are presented. The stability of the rigid-body modes from the LQG compensator is preserved with the auxiliary effect of adding stability to the first elastic mode. The net effect of the ROC is to enhance the stabilizing effect of the LQG compensator at the expense of a reduction of stability robustness margin.

Concluding Remarks

A loop-shaping procedure similar to that used in the LQG/LTR approach was used to design a model-based compensator for the SCOLE configuration, a generic large space structure configuration conceived for the purpose of evaluating and comparing control and identification approaches. Initially, the inputs of a full 26th-order SCOLE model were scaled to avoid numerical difficulties. A 12th-order controller design model was afterwards constructed from the full-order model using modal truncation. Applying a modification of the LQG/LTR technique to the design model produced a 12th-order model-based compensator satisfying stability-performance-robustness design conditions. Finally, an order-reduction technique based on stable factorization was used to produce a 10th-order compensator for controlling the full-order model without destabilizing spillover effects. It was noted that order reduction can have beneficial effects on closed-loop stability but may reduce stability robustness margins. Since the SCOLE configuration is representative of many proposed spaceflight experiments, the results and design techniques employed should potentially be applicable to a wide range of large space structure control problems.

References

[1] M. J. Balas, "Trends in Large Space Structure Control Theory: Fondest Hopes, Wildest Dreams," *IEEE Trans. Auto. Contr.*, Vol AC-27, No. 3, June 1982.

[2] L. W. Taylor and A. V. Balakrishnan, "A Mathematical Problem and a Spacecraft Control Laboratory Experiment (SCOLE) Used to Evaluate Control Laws for Flexible Spacecraft," First SCOLE Workshop, NASA Langley Research Center, Hampton, VA, December 4-7, 1984.

[3] Y. P. Kakad, "Dynamics of Spacecraft Control Laboratory Experiment (SCOLE) Slew Maneuvers," NASA CR 4098, October 1987.

[4] S. M. Joshi, "A Modal Model for SCOLE Structural Dynamics," First SCOLE Workshop, NASA Langley Research Center, Hampton, VA, December 4-7, 1984.

[5] A. Emami-Naeini and P. Van Dooren, "Computation of Zeros of Linear Multivariable Systems," *Automatica*, Vol. 18, No. 4, July 1982.

[6] N. Sundararajan, S. M. Joshi, and E. S. Armstrong, "Robust Controller Synthesis for a Large Flexible Space Antenna," *Journal of Guidance, Control, and Dynamics*, Vol. 10, No. 2, March-April 1987.

[7] S. M. Joshi, and E. S. Armstrong, "Design of Robust Line-of-Sight Pointing Control System for the SCOLE Configuration," Proc. 1987 American Control Conference, Minneapolis, MN, June 10-12, 1987.

[8] M. Vidyasagar, Control System Synthesis: A Factorization Approach, MIT Press, 1985.

[9] M. Athans, "A Tutorial on the LQG/LTR Method," Proc. 1986 American Control Conference," Seattle, WA, June 1986.

[10] G. Stein and M. Athans, "The LQG/LTR Procedure for Multivariable Feedback Control Design," *IEEE Trans Auto. Contr.*, Vol. AC-32, No. 2, February 1987.

[11] A. J. Laub, M. T. Heath, C. C. Paige, and R. C. Ward, "Computation of System Balancing Transformations and Other Applications of Simultaneous Diagonalization Algorithms," *IEEE Trans. Auto. Contr.*, Vol. AC-32, No. 2, February 1987.

[12] K. Glover, "All Optimal Hankel-norm Approximations of Linear Multivariable Systems and Their L^{∞}-error Bounds," *Int. J.Contr.*, Vol. 39, 1984.

[13] Yi Liu, and B, D. O. Anderson, "Controller Reduction Via Stable Factorization and Balancing," *Int. J. Contr.*, Vol. 44, 1986.

TABLE I
EIGENVALUES OF A_E

Mode	Eigenvalue*
1	(-0.00524, 1.747)
2	(-0.00591, 1.970)
3	(-0.0513, 5.108)
4	(-0.0224, 7.449)
5	(-0.0387, 12.903)
6	(-0.0898, 29.925)
7	(-0.104, 34.657)
8	(-0.232, 77.165)
9	(-0.243, 80.993)
10	(-0.446, 148.780)

TABLE II
EIGENVALUE* ANALYSIS OF COMPENSATORS

A-HC	A-BF	$\hat{A}$	$\hat{A}_{ROC}$
(-0.126, 0.126)	(-0.0563, 0.101)	(-0.420, 5.125)	(-0.776, 1.876)
(-0.126, 0.126)	(-0.0834, 0.0837)	(-1.038, 2.027)	
(-0.126, 0.126)	(-0.0959, 0.104)	(-0.203, 1.974)	(-0.204, 1.973)
(-0.00524, 1.747)	(-0.178, 1.976)	(-0.0489, 0.184)	(-0.0500, 0.185)
(-0.00591, 1.970)	(-0.905, 1.956)	(-0.197, 0.237)	(-0.197, 0.237)
(-0.0153, 5.108)	(-0.418, 5.130)	(-0.209, 0.210)	(-0.209, 0.210)

TABLE III
EIGENVALUES* OF FULL-ORDER SYSTEM FORCED BY LQG AND REDUCED-ORDER COMPENSATORS

	LQG	ROC
A-BF	(-0.0569, 0.101)	(-0.0550, 0.0998)
	(-0.0834, 0.0837)	(-0.0834, 0.0837)
	(-0.0971, 0.103)	(-0.0960, 0.103)
	(-0.179, 1.976)	(-0.181, 1.975)
	(-0.905, 1.975)	(-0.634, 1.823)
	(-0.418, 5.130)	
A-HC	(-0.122, 0.128)	(-0.122, 0.129)
	(-0.126, 0.126)	(-0.126, 0.126)
	(-0.126, 0.125)	(-0.128, 0.129)
	(-0.00524, 1.747)	(-0.152, 1.752)
	(-0.00591, 1.970)	(-0.00603, 1.970)
	(-0.0153, 5.108)	(-0.0137, 5.109)
ΔG	(-0.0243, 7.449)	(-0.0242, 7.449)
	(-0.0383, 12.903)	(-0.0383, 12.903)
	(-0.0898, 29.926)	(-0.0898, 29.259)
	(-0.104, 34.657)	(-0.104, 34.657)
	(-0.232, 77.165)	(-0.231, 77.165)
	(-0.243, 80.993)	(-0.243, 80.992)
	(-0.446, 148.780)	(-0.446, 148.780)

* Eigenvalues presented in (Real, + Imaginary) format.

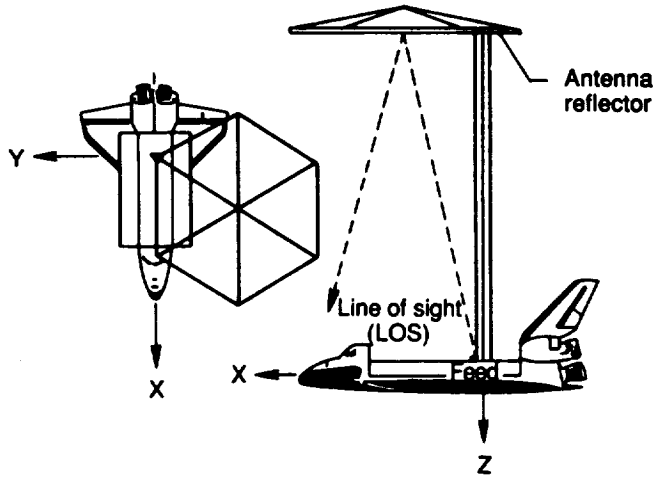

Figure 1. The SCOLE configuration

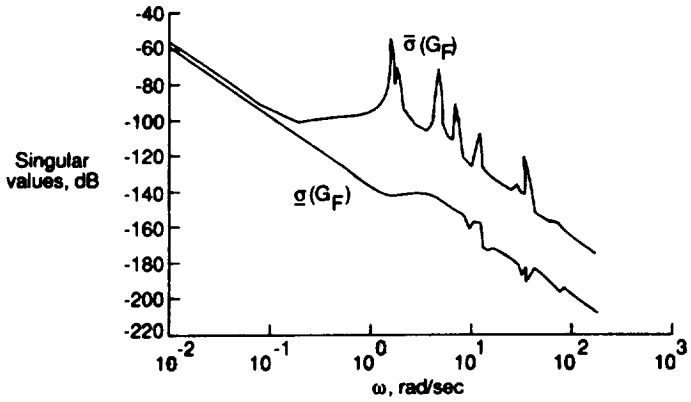

Figure 2. Frequency response of plant after scaling

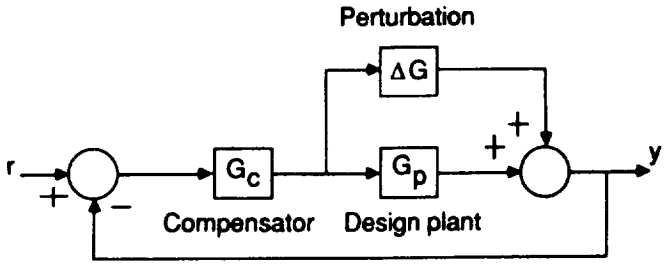

Figure 3. Closed-loop configuration

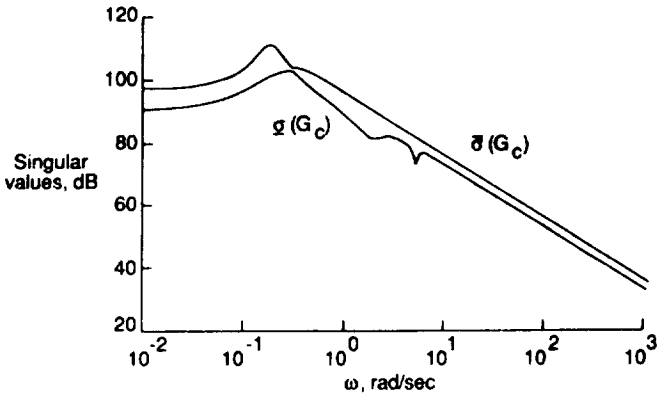

Figure 4. LQG compensator frequency response

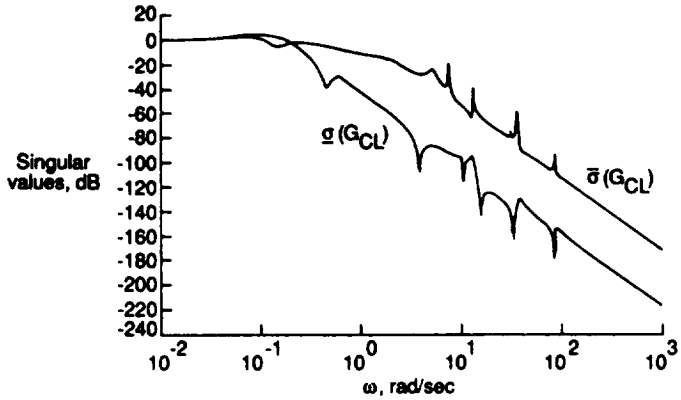

Figure 5. Closed-loop response of evaluation model controlled by LQG compensator

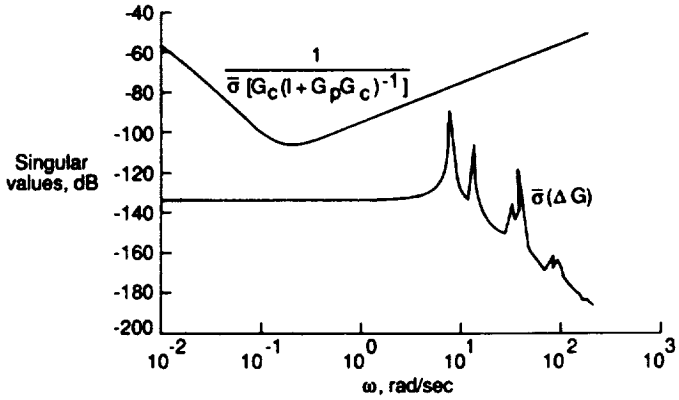

Figure 6. Stability robustness test with LQG compensator

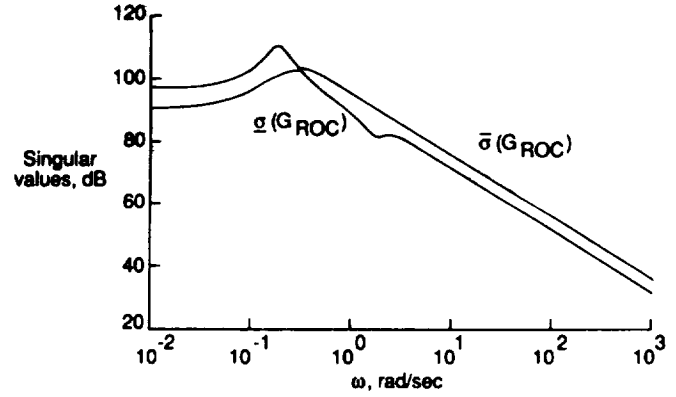

Figure 7. Frequency response of reduced-order compensator

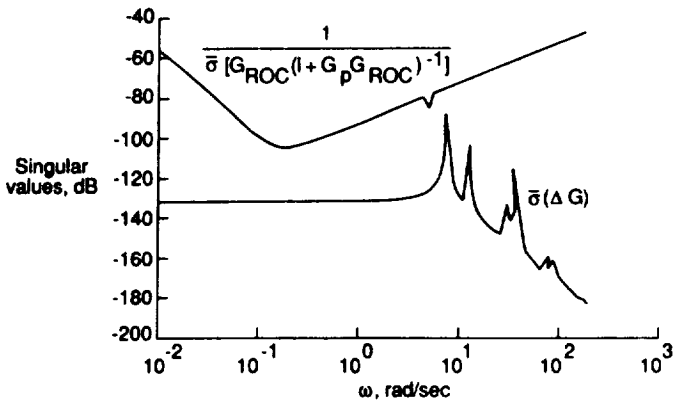

Figure 8. Stability robustness test with reduced-order compensator